Agricultural and Forest Meteorology 173 (2013) 139–153

Contents lists available at SciVerse ScienceDirect

Agricultural and Forest Meteorology

journal homepage: www.elsevier.com/locate/agrformet

Modeling wind fields and fire propagation following bark beetle outbreaks in spatially-heterogeneous pinyon-juniper woodland fuel complexes

Rodman R. Linn[a,*], Carolyn H. Sieg[b], Chad M. Hoffman[c], Judith L. Winterkamp[a], Joel D. McMillin[d]

[a] Earth and Environmental Sciences Division, Los Alamos National Laboratory, Los Alamos, NM 87544, USA
[b] USDA Forest Service Rocky Mountain Research Station, 2500 Pine Knoll Drive, Flagstaff, AZ 86001, USA
[c] Department of Forest and Rangeland Stewardship, Colorado State University, Fort Collins, CO 80523, USA
[d] USDA Forest Service Region 3 Forest Health Protection, 2500 Pine Knoll Drive, Flagstaff, AZ 86001, USA

ARTICLE INFO

Article history:
Received 25 May 2012
Received in revised form 5 November 2012
Accepted 14 November 2012

Keywords:
Heterogeneous woodlands
Bark beetle tree mortality
Fire behavior
FIRETEC
Wind turbulence

ABSTRACT

We used a physics-based model, HIGRAD/FIRETEC, to explore changes in within-stand wind behavior and fire propagation associated with three time periods in pinyon-juniper woodlands following a drought-induced bark beetle outbreak and subsequent tree mortality. Pinyon-juniper woodland fuel complexes are highly heterogeneous. Trees often are clumped, with sparse patches of herbaceous vegetation scattered between clumps. Extensive stands of dead pinyon trees intermixed with live junipers raised concerns about increased fire hazard, especially immediately after the trees died and dead needles remained in the trees, and later when the needles had dropped to the ground. Studying fire behavior in such conditions requires accounting for the impacts of the evolving heterogeneous nature of the woodlands and its influence on winds that drive fires. For this reason we used a coupled atmosphere/fire model, HIGRAD/FIRETEC, to examine the evolving stand structure effects on wind penetration through the stand and subsequent fire propagation in these highly heterogeneous woodlands. Specifically, we studied how these interactions changed in woodlands without tree mortality, in the first year when dried needles clung to the dead trees, and when the needles dropped to the ground under two ambient wind speeds. Our simulations suggest that low wind speeds of 2.5 m/s at 7.5-m height were not sufficient to carry the fire through the discontinuous woodland stands without mortality, but 4.5 m/s winds at 7.5-m height were sufficient to carry the fire. Fire propagation speed increased two-fold at these low wind speeds when dead needles were on the trees compared to live woodlands. When dead needles fell to the ground, fine fuel loadings were increased and ambient wind penetration was increased enough to sustain burning even at low wind speeds. At the higher ambient wind speeds, fire propagation in woodlands with dead needles on the trees also increased by a factor of $\sim$2 over propagation in live woodlands. These simulations indicate that sparse fuels in these heterogeneous woodlands can be overcome in three ways: by decreasing fuel moisture content of the needles with the death of the trees, by moving canopy dead needles to the ground and thus allowing greater wind penetration and turbulent flow into the woodland canopy, and increasing above-canopy wind speeds.

1. Introduction

Pinyon-juniper (*Pinus edulis-Juniperus* spp.) woodlands in the southwestern U.S. are extensive, covering >20 million ha in the region (Miller and Wigand, 1994). These woodlands are characterized by sparse surface fuels and discontinuous tree canopies that can curtail fire spread under low wind conditions (Floyd et al., 2008; Huffman et al., 2009; Miller et al., 2000; Romme et al., 2009). Extensive outbreaks of native bark beetles in recent decades have impacted coniferous ecosystems from Mexico to Alaska, including pinyon-juniper woodlands in the southwestern US (Bentz et al., 2009). A severe drought in 2002–2003 and the associated pinyon ips (*Ips confusus* LeConte) outbreak resulted in the mortality of a large number of pinyon trees across the southwestern US (Breshears et al., 2005; Shaw et al., 2005). The implications of such a large scale mortality event, although largely speculative in nature, are that they increase the potential for large, high-severity fires, especially given parallel trends of earlier and longer fire seasons in many coniferous forest types (Westerling et al., 2006) and projections of warmer and drier climates in the future (IPCC, 2007). Understanding the various physical mechanisms and interactions through which widespread bark-beetle outbreaks and the

* Corresponding author. Tel.: +1 505 665 6254; fax: +1 505 665 3285.
E-mail addresses: rrl@lanl.gov (R.R. Linn), csieg@fs.fed.us (C.H. Sieg), c.hoffman@colostate.edu (C.M. Hoffman), judyw@lanl.gov (J.L. Winterkamp), jmcmillin@fs.fed.us (J.D. McMillin).

0168-1923/$ – see front matter © 2012 Elsevier B.V. All rights reserved.
http://dx.doi.org/10.1016/j.agrformet.2012.11.007

resulting tree mortality alter fire behavior is important in order to inform future decisions about fire risk and fuels management in affected areas.

Two of the effects of tree mortality resulting from bark beetles are (1) the transition of foliage from live to dead fuels and an associated reduction in moisture content, and (2) changes in fuel arrangement when needles fall to the ground. Fire hazard is thought to increase immediately after mortality, when the dead and dry canopy fuels are present (Hicke et al., 2012; Jenkins et al., 2012; Keane et al., 2008), due to the decreased energy required to ignite the fuel and resulting in an increased rate of spread (Page and Jenkins, 2007a; Romme et al., 2006; Schmid et al., 1992; Simard et al., 2010). However, as Hicke et al. (2012) review points out, the implications of fire hazard and propagation in this early-outbreak stage are not well understood. There also exists the notion that after the needles from killed trees have fallen to the surface, the resulting increase in surface fuels can lead to increased surface fire spread, which can in turn result in ignition of the remaining living trees (Allen, 2007). However, understanding changes in fire behavior related to needle fall is complex because both wind flows within the canopy and the spatial arrangement of the fine fuels are altered. It is thus important to account for vegetation/atmosphere/fire coupling when trying to understand the impacts of bark-beetle mortality on fire behavior.

In this paper we use HIGRAD/FIRETEC, a physics-based coupled fire/atmosphere model, to explore fire/vegetation/atmosphere interactions associated with a drought-induced *Ips* beetle outbreak and massive pinyon pine die-off in pinyon-juniper woodlands in northern Arizona. Our objectives were to examine changes in within-stand wind behavior and fire propagation associated with three time periods: in woodlands without tree mortality, in the first year when dried needles clung to the dead trees, and when the needles dropped to the ground. Two ambient wind speeds were used for these studies.

2. Background

The majority of research concerning the impacts of bark-beetle outbreaks on stand structure and fire behavior has been conducted in lodgepole pine (*Pinus contorta*), Douglas-fir (*Pseudotsuga menziesii*), and Engelmann spruce (*Picea engelmannii*)-subalpine fir (*Abies lasiocarpa*) forests (Derose and Long, 2009; Hoffman, 2011; Hoffman et al., 2012a,b; Jenkins et al., 2008; Page and Jenkins, 2007a; Romme et al., 2006; Simard et al., 2010). One exception is Hoffman et al. (2012a), who quantified impacts of bark beetles on ponderosa pine (*Pinus ponderosa*) fuel complexes but did not assess the impacts on fire behavior. Another is Clifford et al. (2008), who provided observational data on fuel complexes and preliminary fire behavior following a pinyon ips outbreak in pinyon-juniper woodlands in New Mexico, but did not attempt to account for spatial variability in the fuels complex or winds. Vegetation/atmosphere/fire coupling is closely tied to the structure of forests and woodlands, which controls both the fire and the wind penetration into the canopy. Fires in pinyon-juniper woodlands, which have highly discontinuous canopy and surface fuels, should not be assumed to burn in the same manner as in forest types that have more continuous canopy or surface fuels.

The distribution and condition of the impacted fuels complexes, and likely thus the potential fire behavior, continue to evolve over time scales of years to tens of years after bark-beetle outbreaks (Hicke et al., 2012). This evolution can be considered in terms of three broadly simplified time periods. The first period is pre-outbreak, when trees are alive with green needles intact. The second period occurs in the first few years following a bark-beetle outbreak, and can be characterized by dramatic changes in fuel-moisture content as green needles on attacked trees die and their moisture levels drop to equilibrate with environmental conditions. The third time period is characterized by changes in fuel distribution as needles fall to the ground, which reduces canopy fuel continuity and oftentimes results in quite heterogeneous fuels complexes depending on the mixture of host and non-host species and the infestation patterns. As the needles fall to the ground, canopy-fuel loading and thus wind resistance within the crowns decreases, but surface-fuel loading increases (Page and Jenkins, 2007b). During this time period greater surface-fuel loading combined with greater penetration of ambient winds could increase surface fire spread under homogeneous stand conditions (Jenkins et al., 2008). However, the potential for the crown-fuel layer to support active fire spread is thought to decrease compared to pre-outbreak levels (Derose and Long, 2009; Jenkins et al., 2008; Page and Jenkins, 2007a; Simard et al., 2010).

Wind flows within forest canopies have been studied by a number of researchers using in situ and wind-tunnel measurements as well as numerical modeling tools; a description of some of these efforts in the context of this paper is provided in Appendix 1. Generally, shear and turbulent mixing are generated due to the interaction between fast moving air above the canopy top and canopy obstructions. The strength of the shear and mixing as well as the momentum exchange between winds above the vegetation and those within the canopy are affected by the scale and magnitude of canopy heterogeneities (Dupont and Brunet, 2006).

Changes in the dynamics of wind penetration through highly discontinuous woodlands have not been well characterized. Yet, it seems likely that modification of the turbulent mixing and coherent vortices that control the injection of horizontal momentum into the canopy, and the resulting shear profile within the canopy post-insect attack would combine to influence fire propagation. Unfortunately, the lack of either in situ experiments or computational fluid dynamis (CFD) modeling efforts focused on understanding winds in discontinuous vegetation types resembling pinyon-juniper woodlands in the southwestern US have thus far made it difficult to assess the changes in fire behavior that would follow such an outbreak in these ecosystems.

The processes that affect the ignition of unburned trees in front of a fire begin as radiative heat transfer warms the unburned fuel (Fig. 1). As energy is deposited in the unburned tree, the temperature increases and some of the moisture near the surface begins to evaporate; when sufficient net heat has been deposited on the surface, the fuel ignites. The net heat deposition is a balance between the heat deposited and that emitted to its surroundings, as discussed in more detail in Appendix 2.

In pinyon-juniper woodlands, where there is minimal surface fuel between the trees, the probability of fire spreading from tree to tree is dependent on the distance between trees and wind speeds within the canopy. When the flames and combustion gas plumes are angled more vertically, as occurs at lower wind speeds (the flame angle in Fig. 1, θ, increases toward 90°), a shorter distance between trees, d, can be bridged by the propagating fire front. Crossstream-wind fluctuations determine the crossstream range of tree locations that can be heated by an upstream burning tree and the potential of fire spreading from tree to tree in directions other than directly downwind. Both streamwise and crossstream turbulence are affected by the homogeneity of the canopy fuel distribution. Previous studies (Parsons, 2007; Pimont et al., 2011) illustrated that changes in canopy structure, namely aggregation vs. even distribution of canopy vegetation, significantly impact fire spread in thinned treatment zones in dense pine stands with heavy and continuous surface fuels. Unfortunately, the results of these studies are not transferrable to pinyon-juniper woodlands, which are characterized by greater horizontal heterogeneity in overstory and surface fuels.

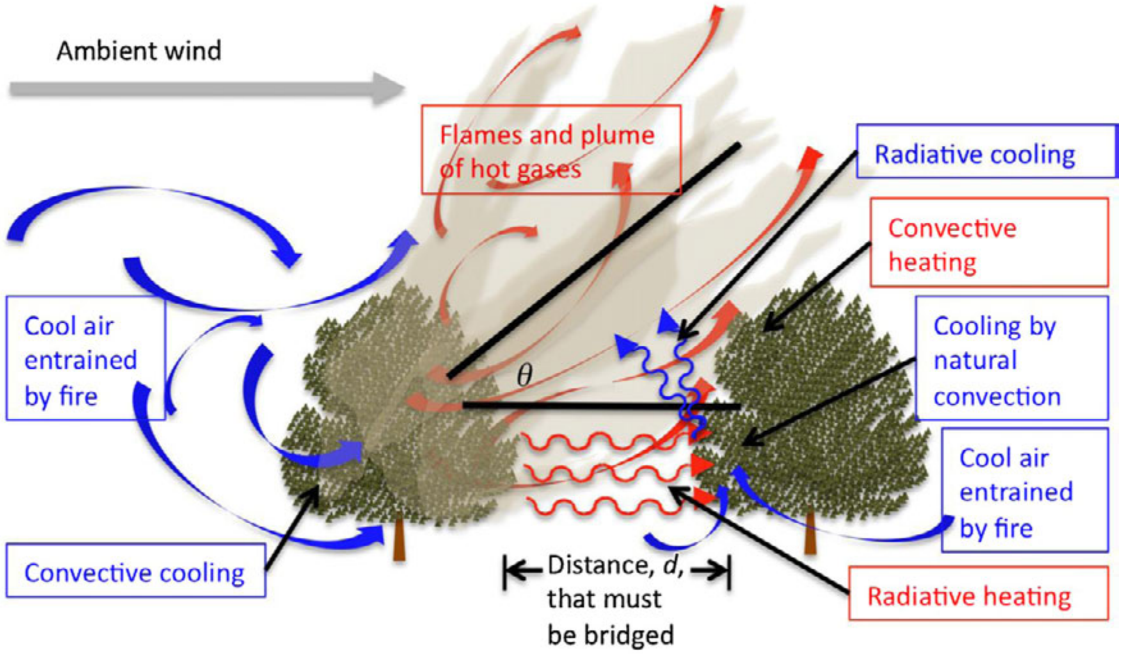

Fig. 1. Simplified conceptual model of the processes that control the spread of fire to unburned vegetation in discontinuous woodland ecosystems.

Previous studies have quantified post-outbreak changes in stand structure and fuels complexes, and then assessed fire-behavior changes at stand levels, primarily using point-functional quasi-physical fire models based on linkages between Rothermel's (1972, 1991) surface and crown fire spread models or Van Wagner's (1977) crown fire initiation and spread models. Modeling systems based on these linkages do not directly account for the effects of fuel discontinuities on temporal and spatial variability in wind flow and fire spread at landscape scales. The assumption of homogeneous fuels complexes, which is made in these models, is particularly tenuous for mixed-species situations such as pinyon-juniper woodlands where bark beetles kill only one species and surface fuels are patchy. In addition to assumptions related to homogeneity, Cruz and Alexander (2010) have challenged the use of Van Wagner's (1977) crown-fire model in scenarios with fuel moisture <70%, such as in the case where the canopy needles are dead yet still on the trees. In pinyon-juniper woodlands, during the 2002 severe drought in New Mexico, fuel moistures of dead pinyon needles were <20% (Stimson et al., 2005).

Recently developed process-based fire models, such as Wildland-Urban-Interface Fire Dynamics Simulator (WFDS) (Mell et al., 2007, 2009) or HIGRAD/FIRETEC (Linn, 1997), hereafter referred to as FIRETEC, account for the spatial structure of fuels. Models like WFDS and FIRETEC use CFD techniques and three-dimensional (3D) grids to describe evolving, spatially varying quantities such as temperature, velocity of gaseous species and various characteristics of the fuel. Such models represent vegetation as a porous medium that provides bulk momentum and heat exchange terms between the gas and solid phases. Fuel is described by assigning mean or bulk quantities such as fine-fuel surface area per unit volume, moisture content, and density to each computational cell in the 3D grid. This methodology facilitates simulating fires in areas with complex fuel beds that are vertically and horizontally heterogeneous.

One of the advantages of models such as FIRETEC or WFDS, which were developed based on a general representation of the physical processes that drive a fire, is that they can be used to suggest possible ramifications of such process interactions even if they extend beyond the conditions for which we have experiments. However, it is important to keep in mind that they are still just models of reality, and simulation results should be used with caution. Simulation tools such as these can reasonably be used to suggest possible ways that physical phenomena will interact under various environmental conditions to cause a nonlinear fire response. Such suggestions should drive new experiments, field observations or data analysis to verify the model-driven hypotheses. With this perspective in mind, this work explores potential ways that drought/insect-driven disturbance of heterogeneous fuel complexes (such as pinyon-juniper woodlands) could drive changes in wind penetration into the forest canopy, subsequent coupled fire/atmosphere interactions, and fire spread.

3. Methods

3.1. Simulation fuel beds

We populated a 400-m × 400-m domain with a heterogeneous fuels complex based on field data collected in 2009 on 48 permanent plots established in three National Forests (Kaibab, Coconino, and Apache-Sitgreaves) in Arizona following the severe pinyon pine die-off in 2002–2003. We quantified stand structure and surface fuels in plots with and without pinyon pine mortality using methods outlined in Hoffman et al. (2012a). We then used the field data to create a single realistic fuel bed to represent pinyon-juniper woodlands in the southwestern United States and focused on the likely evolution of that fuel bed over the three simplified stages of stand conditions following an outbreak. Amongst the range of site conditions measured by Hoffman et al. (2012a), we chose to simulate a fuel bed whose tree density and mortality were near the higher end of the measured distributions in order to study those conditions that are of most concern to fire and fuels managers. The simulated fuels complex had a tree density of ~1000 trees ha^{-1} comprised of 77% pinyon and 23% juniper trees based on plot averages. SpPack, an Excel macro (Perry, 2004), was used to randomly determine tree spatial locations within the domain.

We used an approach similar to one outlined in Linn et al. (2005b) to distribute the fine fuels within the randomly-placed trees, whereby a series of parabolic profiles were used to describe

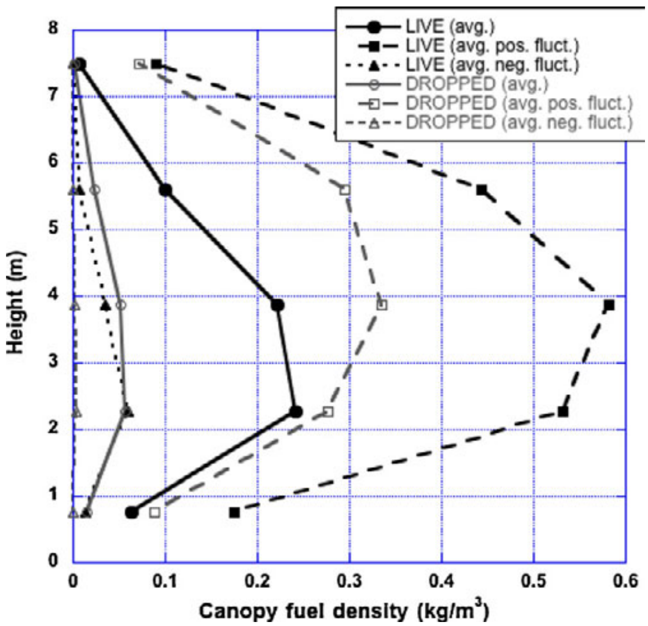

Fig. 2. Canopy fuel density fluctuations (average, average positive, and average negative) as a function of height for pinyon-juniper woodlands before a severe pinyon ips outbreak (LIVE), and following the outbreak when the dead needles have fallen to the ground (DROPPED).

the distribution of fine-fuel density based on the tree's attributes and distribute mass into computational cells. Fuel mass distributions were comprised of fine fuels (needles and twigs <2 mm), since larger materials contribute little to the combustion process at the fire front (Rothermel, 1983). The simulation domain is a 3D array of computational cells that are 2 m on horizontal sides and about 1.5 m in height near the ground (the cells stretch with height).

Surface fuels were distributed across the simulation domain using a methodology similar to Linn et al. (2005b), such that litter (needles and fine woody fuels) was concentrated under tree canopies and decreased exponentially away from the center of the trees, whereas herbaceous fuels were concentrated in openings, decreasing exponentially under the trees.

To explore the possible evolution in fire behavior as a result of bark beetle attack, simulations were performed for three time periods surrounding the attack: (1) before the bark beetle attack ("LIVE"); (2) 100% mortality of the pinyon, with cured needles on the trees ("DEAD"); and (3) 100% mortality of the pinyon, with needles on the ground ("DROPPED"). In the LIVE simulations we set the crown foliage moisture at 80%, which represents severe fire conditions in the southwestern US (Roccaforte et al., 2008). In the DEAD simulations, the foliage-moisture content of the juniper trees was 80% whereas the foliage-moisture content of the dead needles on the pinyon trees was 15%. In the DROPPED simulations, needle biomass from the dead pinyon trees was translated downward, contributing to the litter in the surface cells under the trees. The moisture content of litter and grass fuel load was 5% in each of the simulations, representing drought conditions during fire season in the Southwest. In all scenarios, the trees (dead or alive) are in the same locations. The topography was flat with zero slope.

The simulations were characterized by large variations between stand average densities at a given height and densities within the trees (average positive density fluctuations) and in the gaps between the trees or on the edges of a tree (average negative density fluctuations). The ratio of average positive fluctuation to average density is larger as the forest becomes sparser, such as seen in the DROPPED stand compared to the LIVE stand (Fig. 2). These variations were much higher than those that characterize more continuous forests.

3.2. Simulation wind fields

Observations (Romme et al., 2009) and simulation-based studies (Simard et al., 2010) in lodgepole pine forests suggest that under low winds and relatively high fuel moistures, few stands burn; whereas, at higher wind speeds and lower fuel moistures, most stands burn regardless of whether or not they were attacked by bark beetles. Therefore, for this study, fires were simulated under moderate ambient wind conditions to explore the effects of bark beetle attacks in regimes where the fire might propagate but was not likely to burn independent of fuel conditions (as suspected for extreme wind conditions). Two different aloft wind speeds, 24 m/s and 12 m/s at a height of 450 m (referred to as HIGH and LOW respectively, even though both can be considered moderate) with neutral atmospheric conditions were used to generate two wind fields for each of two vegetation stages (LIVE and DROPPED). The wind fields for the LIVE and DEAD canopies were assumed to be the same because the fuel distributions are the same. The differences in water mass associated with the transition from LIVE to DEAD conditions are assumed to not change the wind field significantly because the volume of the fuels is assumed to be the same. The effect of the changes in mass of the foliage on the drag is neglected as we are neglecting the dynamic response (movement) of the trees in these moderate to low winds. We did not consider the differential effects caused by changes in albedo or evapotranspiration when the needles die and change color.

Appropriate initial and boundary condition wind fields, including both the mean velocities and turbulent fluctuations, were developed for the LIVE and DROPPED stands by precomputing wind fields in the manner described in Pimont et al. (2011) and Cassagne et al. (2011). With this methodology, winds are simulated with cyclic boundary conditions on all lateral boundaries without the presence of fire in the domain. Wind profiles generated in this manner evolve toward a balance between the effects of the atmosphere aloft, the heterogeneous aerodynamic drag and the turbulence generated in/by the stand. These wind simulations produce a dynamic series of wind fields that reflect these balances, and are used as inlet boundary and initial conditions for the fire simulations.

It is difficult to simulate fires in the various stages after a bark beetle attack with the "same" winds because variations in canopy structure alter the wind patterns. It is important to recognize that even though both of the HIGH (LIVEHIGH or DROPPEDHIGH) wind conditions have similar wind speeds far above the canopy (e.g. 100 m height), the wind speeds within and just above the canopy for these HIGH scenarios will be different between the LIVE and DROPPED fuel beds, and similarly for the LOW wind conditions. Thus, functional relationships between rate-of-spread (ROS) and wind speed at a given height, $U(z)$, will have different dependencies on height, z, for different stand structures. The wind profiles dictate the way the spread-rate/wind-velocity correlations change depending on the height at which the winds are measured as described in Linn and Cunningham (2005), but in this case there is additional complexity due to the fact that the wind profiles change with stand structure. Turbulence statistics for the non-fire-influenced winds were generated by averaging these winds over a 10-m wide (streamwise or x-direction) strip near the inlet, across the width of the domain in the crosswind (or y-direction), for 400 s of the wind simulations.

In this study the fire was ignited 100 m from the upwind boundary along a 100 m long straight line. Fire propagation distance is determined once per second as the farthest downwind surface location where the resolved fuel temperature exceeded 500 K. Mean

Table 1
Average wind speeds (m/s) at the top of canopy, U_0 (7.5 m height) for four simulations.

Simulation	U_0 (m/s)	Speed-up factor ($U_0/U_{0,\text{Live}}$) (m/s)
LIVELOW	2.52	1
DROPPEDLOW	3.57	1.42
LIVEHIGH	4.49	1
DROPPEDHIGH	6.36	1.42

ROS is estimated as the slope of a least squares fit to the propagation distance vs. time curves.

The crosswind extent of the fire was calculated using a method similar to that used for the propagation distance, namely distance between the farthest extent to the left and right where fuel temperatures exceeded 500 K. This should be considered the projection of the burning fireline in the crosswind direction and not the length of the fireline, since it does not include the fireline curvature or the streamwise components of the fireline. A measure of the active crosswind-fireline length is found by counting the number of computational x–z planes in the domain that have one or more cells with fuel temperatures above 500 K. The difference between the active crosswind fireline length and the crosswind extent indicates the degree to which the fireline is discontinuous or has holes that are not intensely burning.

The heat release rate is a function of the size of the fire and fraction of the fire perimeter that continues to burn. Since our simulated fires spread at different speeds and had different shapes, comparison of heat release rates at any single point in time is difficult to interpret. Therefore, we chose to look at the evolution of the integrated heat released by the fire as it progressed. This integrated heat release can be thought of as fire intensity integrated over time and fire perimeter. It was calculated for each of the simulations by summing up the total heat that had been released up to a given point in time in the simulation. A derivative metric of integrated heat release rate was calculated by performing a least squares fit to the integrated heat release vs. time curve to get an average heat release rate (AHRR).

4. Results

4.1. Ambient winds

As suggested above, the ambient velocities within the various stands are different (Table 1). The speed-up factor for winds at the top of the canopy is the ratio of the wind speed of the DROPPED case to that of the LIVE case. The similar value of 1.42 for both the HIGH and LOW wind cases suggests that at least over this range of wind speeds, the wind speed-up factor due to needles falling to the ground is not a strong function of wind speed above the canopy. Thus, it is reasonable to normalize the velocities within the canopy by U_0, as shown in the raw and normalized streamwise wind profiles of Fig. 3a and b.

The presence of the needles on the pinyon trees affects both the magnitude of the mean wind speed as well as the shape of the velocity profile in the canopy (Fig. 3a and b). The normalized velocity profiles for the HIGH and LOW wind cases are remarkably similar, even though the non-normalized magnitudes are not similar. As expected, below the top of the canopy the normalized wind speeds are slower in the LIVE cases, where the needles are on the trees, than the DROPPED cases for both HIGH and LOW winds. The LIVE cases have a higher velocity gradient near the top of the canopy than the DROPPED cases, and therefore normalization results in higher normalized velocities above the top of the canopy.

In the LIVE cases, the shapes of the trees and slightly wider spaces between trees with foliage near the ground vs. mid canopy lead to a slightly higher wind speed at .75 m than at 2.26 m above the ground (Fig. 3a). This feature does not exist in the DROPPED wind profiles, where the canopy is more open, so the flow through the canopy is less restricted and more thoroughly mixed (Fig. 3b).

The vertical mixing that brings kinetic energy from the ambient winds above the canopy down into the canopy is related to turbulent-velocity fluctuations in the atmosphere, which are affected by the velocity gradient near the top of the canopy. Fig. 3c–e illustrate the average of the normalized square of the fluctuations in the U, V and W velocities (x, y, and z components of the velocity vector), where these velocities are decomposed into mean and fluctuating parts, such as $U = U' + \bar{U}$. Half of the sum of these three averages is frequently referred to the normalized turbulent kinetic energy, which is a measure of the kinetic energy associated with the fluctuations or turbulence compared to the mean flow. In the LIVE cases, the ratio of the u-velocity fluctuations in the lower portion of the canopy to the velocity at tree height (the normalized velocity in the lower portion of the canopy) is smaller than in the DROPPED cases (Fig. 3c), which is similar to trends in mean velocities (Fig. 3b). In the upper portion of the canopy, the LIVE normalized u-velocity fluctuations are larger than those in the DROPPED case, similar to mean velocities calculated above the top of the canopy. Fig. 3c–e illustrate that the strength of the fluctuations in the crosswind and vertical directions are approximately half and one fourth as strong as the velocity fluctuations in the streamwise direction, which is indicative of anisotropic turbulence and thus mixing.

The normalized cross correlation (Fig. 3f) is indicative of the strength of the vertical mixing that transports streamwise momentum down into the canopy, and is larger in the LIVE cases than the DROPPED cases. This is consistent with the larger sink to streamwise momentum due to drag in the LIVE cases. In order to develop steady state spatially-averaged velocity profiles, the flux of horizontal momentum above the canopy must equal the sink of this momentum due to wind interactions within the canopy.

The instantaneous velocity patterns in Fig. 4 provide another illustration of the wind variations that constitute the turbulence fields. The heterogeneity in these fields is the result of nonlinear interactions between the ambient winds and the discontinuous tree canopy. From Fig. 4, it is apparent that the turbulence in the LIVELOW case is not isotropic since the three components of the velocity do not show the same relative magnitude of variations. In addition to the difference in magnitude of the u, v, and w variations, the nonisotropy of the turbulence structures is apparent with the more elongated patterns in the streamwise direction (u) compared to the other components. The HIGH velocity wind cases and winds in the DROPPED fuel beds show similar patterns and trends, but different magnitudes and ranges.

4.2. Fire propagation

The rate of fire propagation varied among the simulations, becoming extinguished in some scenarios (Fig. 5). In the LIVELOW simulation (Fig. 5a), the fire is nearly extinguished and has stopped propagating. This fire initially propagates from the ignition line, but quickly breaks up into several disjunct pieces due to a combination of the heterogeneous wind field and discontinuous fuel bed. In the LIVEHIGH simulation (Fig. 5b) in the same vegetation stand, but with wind speeds at the top of the canopy about 1.8 times faster than LIVELOW, the fire is able to propagate in most locations along the fireline, although in one location the fireline becomes disjunct owing to local fuel arrangement. Higher lateral wind fluctuations in the LIVEHIGH as compared to LIVELOW scenario contributed to the difference in fire behavior in these two simulations (Fig. 5a and b). These lateral fluctuations enhance the ability of the fire to move forward in a diagonal fashion instead of

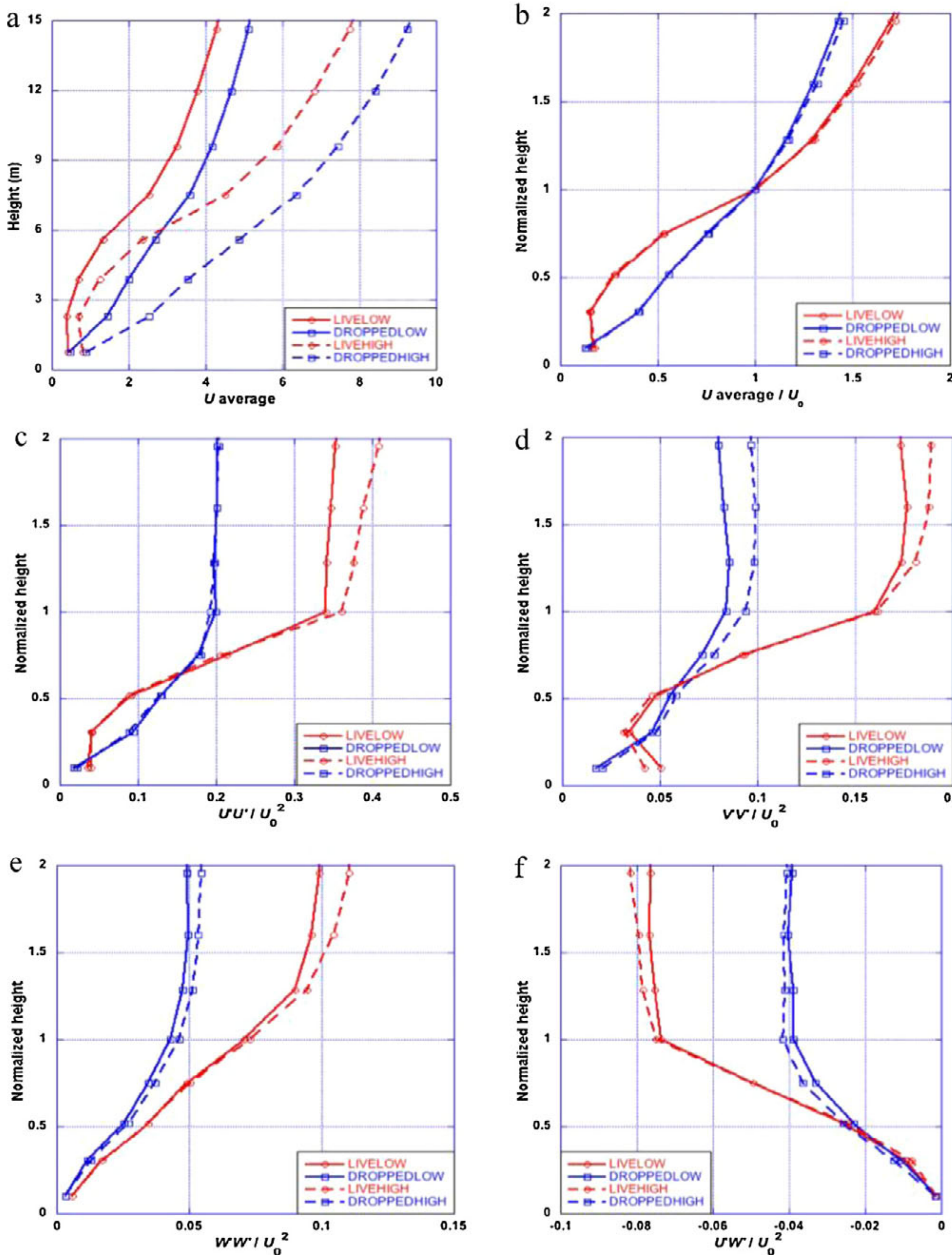

Fig. 3. Vertical profiles of: (a) streamwise wind speed, U, (b) normalized streamwise wind speed, U/U_0 (c) normalized streamwise velocity correlation, $\overline{U'U'}/U_0^2$, (d) normalized crossstream velocity correlation, $\overline{V'V'}/U_0^2$, (e) normalized vertical velocity fluctuations, $\overline{W'W'}/U_0^2$, and (f) normalized vertical/streamwise cross correlation, $\overline{U'W'}/U_0^2$, for LIVELOW (solid red), DROPPEDLOW (solid blue), LIVEHIGH (dashed red), and DROPPEDHIGH (dashed blue) scenarios. Height is normalized by H, which is approximately 7.5 m (nominal height of the canopy).

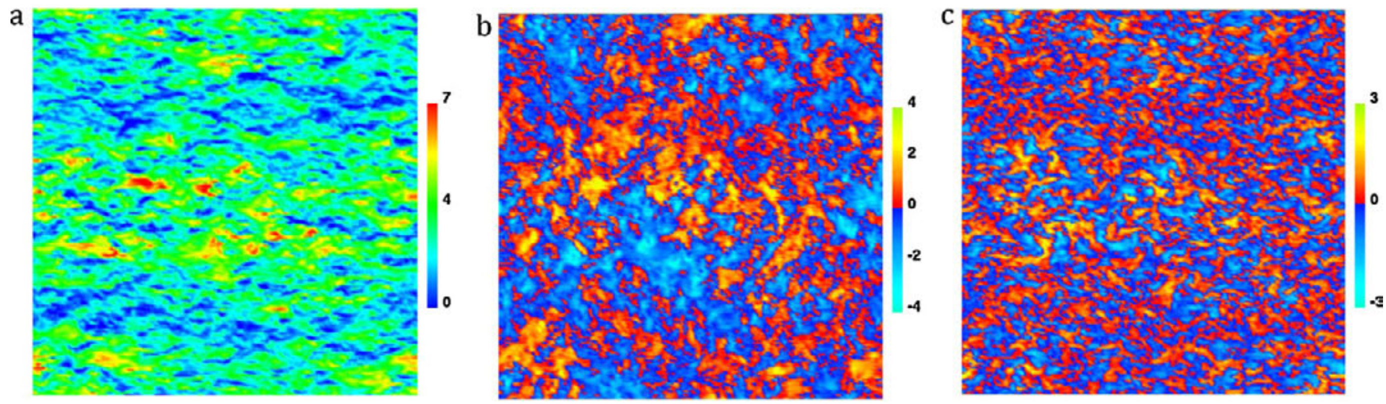

Fig. 4. Horizontal slices showing three velocity components from the LIVELOW simulation at $z = 7.5$ m: (a) u (dark blue is $u = 0$ m/s and red is $u = 7$ m/s), (b) v (light blue is $v = -4$ m s^{-1} and yellow is $v = 4$ m/s), (c) w (light blue is $w = -3$ m/s and yellow is $w = 3$ m/s). In these slices, inlet winds enter the domain from the left. The x axis is left to right and y axis is bottom to top in these images.

being constrained to just moving downwind, as occurs when there are minimal lateral fluctuations.

In the DEADLOW simulation, even with the same upwind wind field was used for the LIVELOW simulation, the reduced crown moisture in the pinyon trees allows the fire to propagate (Fig. 5c). The faster spreading DEADHIGH fire (Fig. 5d) also benefits from the lower moisture in the pinyon crowns. Additionally, increased streamwise winds associated with the HIGH wind scenario push the combustion gases into the unburned fuel with higher efficiency than in the LOW scenario.

Reduced canopy fuel loading, less canopy fuel continuity (larger spaces between trees with fine canopy fuels) and increased surface fuels all contribute to increased fire propagation in the DROPPEDLOW and DROPPEDHIGH scenarios (Fig. 5e and f) over the LIVE cases. It is noteworthy that because we assumed that the pinyon needles fall straight down to the ground, the continuity of the surface fuels is not modified and gaps in surface fuels between trees are not filled in. This is markedly different than operational models that assume that increases in fuel loadings result in a homogeneous increase in surface fuel loads across the simulated domain. The

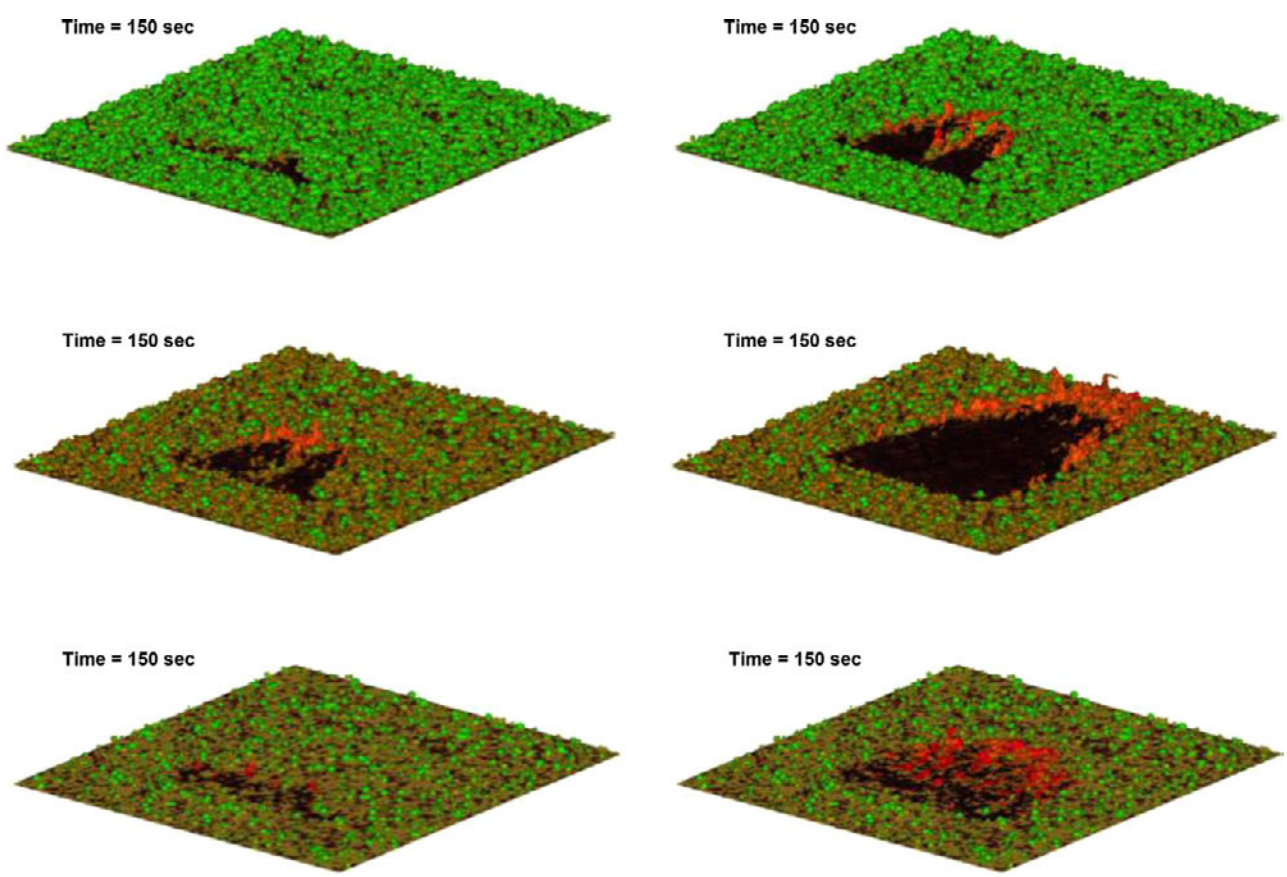

Fig. 5. Simulations at 150 s after ignition: (a) LIVELOW; (b) LIVEHIGH; (c) DEADLOW; (d) DEADHIGH; (e) DROPPEDLOW; and (f) DROPPEDHIGH. Colors on the horizontal plane indicate bulk surface fuel densities. Live tree locations are shown in green, dead tree locations are shown in brown. Areas of the canopy that have been significantly burned are shown in black. The orange, red, and gray isosurfaces indicate areas of hot gases.

Table 2
Normalized velocity and fire rates-of-spread (ROS).

Simulation	Average wind speed at top of canopy, U_0 (m/s)	Mean fire spread rate, ROS (m/s)	Normalized fire spread rate, ROS* (ROS/U_0)	ROS*/ROS*$_{LIVE}$
LIVELOW	2.52	0.322	.127	1
DEADLOW	2.52	0.830	.329	2.59
DROPPEDLOW	3.57	0.40	.112	.882
LIVEHIGH	4.49	1.09	.243	1
DEADHIGH	4.49	2.00	.445	1.83
DROPPEDHIGH	6.36	1.38	.217	.893

impacts of various spatial arrangements of surface fuels are left for investigation in future work.

In Fig. 6 the fire-propagation distance curve for LIVELOW stops at approximately 120 s or 42 m because the fire went out and ceased propagating, whereas the fire in the DEADLOW scenario continues to propagate until the end of the simulation. As expected, the ROS for the HIGH wind cases are faster than those for the LOW wind cases using the same fuel bed, and the DEAD simulations have faster spread rates than the LIVE simulations (Table 2). Less intuitive is the result showing that fires are more robust and move slightly faster in the DROPPED simulations than the LIVE simulations with the same wind speed at 100 m altitude, even though there are less canopy fuels in the DROPPED scenario (see Fig. 5). It is important to remember that the wind speeds in the canopy are not the same for these LIVE and DROPPED cases.

ROS is often described as being a function of wind speed. As discussed above, the various fuel beds create different local wind fields within the fuel bed, thus complicating the direct comparison of spread rates even between the various HIGH or LOW wind cases. Normalizing ROS by U_0 (ROS* in column 4 of Table 2) allows for more direct comparison of ROS between scenarios with LIVE and DROPPED fuel beds, and accounts for the varying winds found at the top of the canopy for the different fuel structures.

The ratio of the normalized rate of spread, ROS*, to the ROS* for the LIVELOW or LIVEHIGH case, as appropriate for the wind regime of the simulation, (see column 5 of Table 2), provides a measure of the impacts of the reduced pinyon foliage moisture in the DEAD simulations and the combined drying and redistribution of needles in the DROPPED cases. It is important to note that even though the ROS* decreased in the DROPPED cases vs. the LIVE cases, the DROPPEDLOW scenario allows the fire to continue to propagate whereas the LIVELOW case stops propagating and goes out.

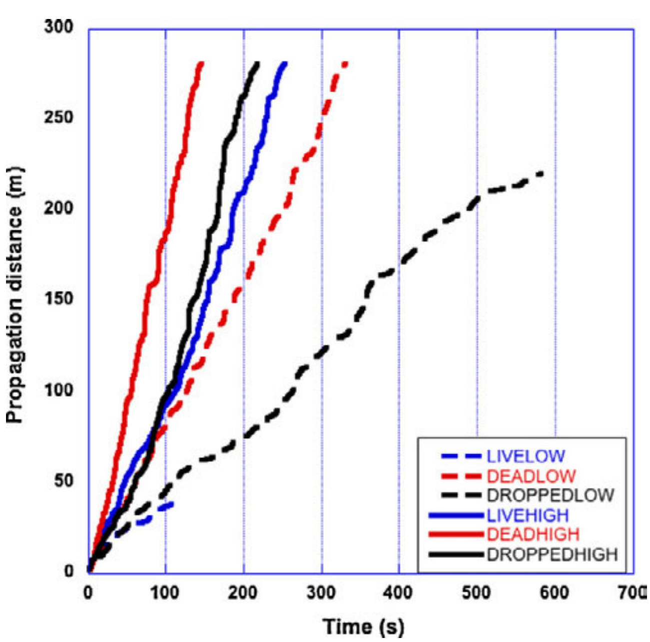

Fig. 6. Propagation distance as a function of time for each of the six simulations.

In Fig. 7a the crosswind extent of burning evolves from the original 200 m length, with the DEADHIGH and DROPPEDHIGH fires becoming wider from the left to right flanking edges. In contrast, the lateral extent of the fire in the other simulations becomes smaller after the fire moves away from the original ignition line. Abrupt drops in the curves in Fig. 7a indicates that the firelines are being fragmented and one of the fragments on either the left or right flank of the fire ceases to actively burn; thus, the lateral or crosswind extent of the fireline is abruptly reduced. Increases in the values of the curves in Fig. 7a indicate the left and right flanking edges of the fire are diverging from one another.

In the first 50 s after ignition there are gaps or discontinuities in all of the simulated firelines. This is shown in Fig. 7b by the crosswind length of active burning being less than the overall crosswind extent of the fires. In all but the DEADHIGH and DROPPEDHIGH fires, the crosswind extent of the fires remains less than the initial ignition length. The LIVELOW fire continues to shrink in its lateral extent as well as the crosswind length of active fireline until eventually there is no active fireline left. In contrast, the LIVEHIGH fire initially develops some gaps immediately after ignition, and at least one end of the fireline is extinguished around 50–75 s into the simulation. The remaining active portions of the fire continue to burn until around 190 s, when one of the remaining active fingers of the fire is extinguished. After 200 s the values of the crosswind extent and crosswind length of active fireline are approximately the same and nearly steady at 150 m long. This indicates that the remaining 150 m of fire is almost continuous with no significant gaps along its length. All of the LOW wind cases have gaps in the firelines that are not actively burning (i.e. they are broken; Fig. 7). Only in the DROPPEDLOW case is a LOW wind fire able to increase in width or heal any of the gaps within its fireline. After some initial adjustments, even the DEADLOW fire begins to burn with an extent of about 130 m that slowly diminishes.

The integrated heat release curves in Fig. 8 show that the shapes of the LOW wind speed curves are relatively straight whereas the HIGH wind speed curves all have a bend occurring shortly after ignition, with steeper slopes thereafter. This difference can be explained by the fireline length and headfire thickness. In the HIGH wind scenarios the flanking portions of the fireline stretch out as the fire propagates and the fireline thickness (or depth in the streamwise direction) increases. In the LOW wind simulations the flanking portions of the fire are limited and the fireline thickness does not grow as much.

The average slopes of the lines in Fig. 8, shown in the second column of Table 3, can be interpreted as the average heat release rate (AHRR) for each fire over its duration. The ratio of the AHRR to the AHRR for the respective LIVE fuel case for LOW or HIGH wind speeds (third column of Table 3) can be interpreted as the factor of increased heat release associated with the needles drying out (DEAD) or with the needles drying out and then falling to the ground (DROPPED). For the DEAD fuel conditions, the ratio of

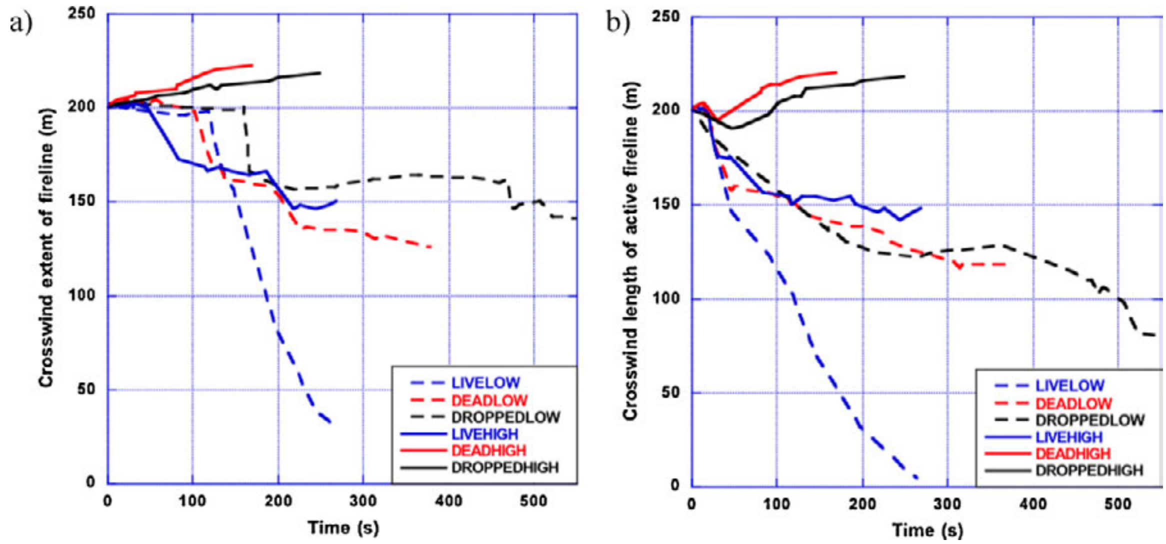

Fig. 7. (a) Maximum crosswind extent of firelines measured from the farthest left flank to the farthest right flank of the fire with active burning (fuel temperatures >500 K); (b) cumulative crosswind width of burning sections that are actively burning.

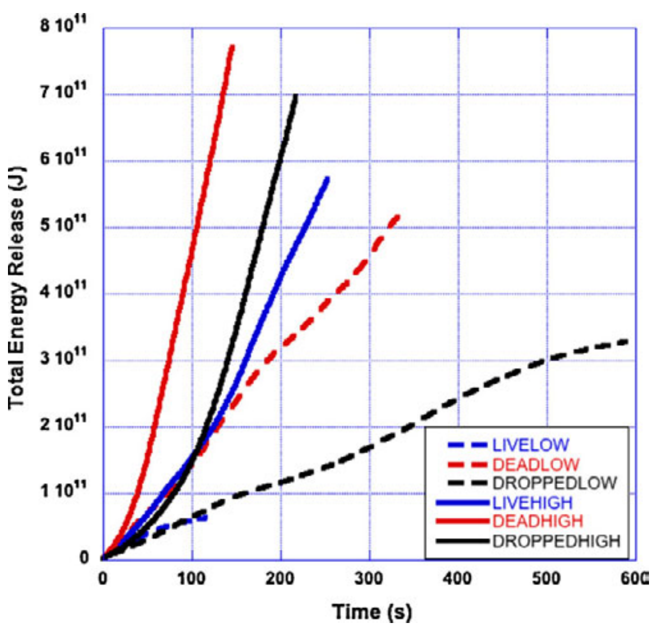

Fig. 8. Integrated heat release (J) for the six simulations.

the increase in intensity was larger in the LOW wind case than in the HIGH wind case, but the reverse is true in the DROPPED fuel conditions. This indicates a complex relationship between the intensity, wind speed, and fuel distribution. The fourth column of Table 3 includes an indicator of the heat released per meter of forward spread, namely the AHRR divided by the average ROS from Table 2. The ~30% difference in the values for LOW and HIGH wind conditions is indicative of longer and less fragmented firelines as well as more complete consumption of fuels in the HIGH wind case.

Table 3
Average heat release rate (AHRR) metrics.

Simulation	Average heat release rate, AHRR (GW)	$AHRR/AHRR_{LIVE}$	AVRR/ROS (GJ/m)
LIVELOW	.50	1	1.6
DEADLOW	1.6	3.2	1.9
DROPPEDLOW	.58	1.2	1.5
LIVEHIGH	2.3	1	2.1
DEADHIGH	5.6	2	2.8
DROPPEDHIGH	3.2	1.4	2.3

5. Discussion

5.1. Wind flow implications of bark beetle mortality

The simulation results illustrate the significance of the change in woodland structure on the penetration of winds into the tree canopy. The fact that opening up or reducing the density of the woodland canopy increases mean wind speed and changes the wind profile shape is consistent with observations and simulation results in previous works (described in Appendix 1). The speed up in the canopy-top winds from the LIVE to DROPPED cases is surprisingly similar, increasing by a factor of 1.42, given the turbulent wind fields and nearly factor of two difference between the LIVEHIGH to the LIVELOW mean wind speed at the top of the canopy. This similarity is demonstrated in the mean wind profiles throughout the canopy, and is consistent with the normalized canopy velocities used in numerous previous works. It suggests that a similar normalization has value when considering the impact of tree mortality on canopy winds.

The mean wind profiles of the LIVE forest have some characteristics similar to the mean wind profiles described in previous works pertaining to flow in more dense canopies, but the DROPPED wind profiles illustrate significant differences from the LIVE profiles. As discussed in Pimont et al. (2011), the precise shape of the profiles depends on the cover fraction and vegetation density, which are different for the pinyon-juniper woodlands than other canopies investigated. In addition, the degree of aggregation of mass into clumps of trees or homogeneously distributed trees (Pimont et al., 2011) also have implications for this study, since the mortality of the pinyon trees results in the canopy fuels distribution being more aggregated (concentrated in the junipers) with wider spaces between the remaining fuels. The difference in mean-wind profiles of the LIVE and DROPPED cases in this study are qualitatively similar to the trend found when comparing less to more aggregated scenarios in Pimont et al. (2011), as well as the effects of reducing the canopy fuel load. This trend is to damp out the inflection of the vertical profile of streamwise velocity (shown in Fig. 3a and b) and lower its height.

The higher normalized turbulence quantities in the LIVE than in DROPPED cases indicates that the flows near the top of the canopy are more intermittent in the LIVE case, and the winds at the top of the canopy in the DROPPED case are more dominated by the mean wind. This is consistent with the fact that the mean DROPPED velocity profile is more similar to the profile expected for a scenario with surface fuels but no canopy than the LIVE case.

The differing above-canopy profile features we observed between LIVE and DROPPED simulations might suggest that: (1) the anisotropic aspects of turbulence intensity and turbulent length scales are affected differently by different canopy structures, and (2) aspects of the streamwise turbulence length scales are controlled by distance between trees in the closer-packed LIVE case whereas they may be more affected by wake structures behind individual trees in the DROPPED scenario. The scales of these wake structures are functions of wind speed in the less-dense DROPPED cases, but are also affected by shorter-distances to nearby trees in the LIVE cases. These issues warrant further investigation but are outside the scope of this paper.

The mixing related to the normalized cross-correlation, $\overline{U'W'}/U_0^2$, is the critical driver keeping the air amongst the trees moving in spite of the aerodynamic drag of the trees that continually slows the wind in the canopy. The negative values that occur in this quantity indicate that the mixing is causing positive fluctuations in the streamwise winds in the canopy when there is a gust of wind moving toward the ground (negative vertical velocity fluctuations). Such negative values are typical for positive vertical gradients in the streamwise direction in previous canopy flow studies such as those mentioned above. The larger magnitude of the values of $\overline{W'W'}/U_0^2$ and $\overline{U'W'}/U_0^2$ in the LIVE woodlands compared to the DROPPED woodlands is due to more drag in the LIVE forests. When there is more drag, there is a stronger velocity gradient near the top of the trees; stronger vertical mixing is more effective at supplying a source of horizontal momentum within the canopy layer.

The slightly negative gradients of streamwise and crosswise components of turbulent kinetic energy in the LIVE cases near the ground are associated with the slightly faster mean velocities below the most dense portion of the canopy (in this setting, where herbaceous fuels that enhance surface drag are scarce.) This feature appears to be a function of canopy structure since the DROPPED cases do not show this feature; we suspect that this is due to the greater mean velocities throughout the canopy in the DROPPED case. It is also possible that in these simulations the flow field under the trees is being under-resolved, thus affecting the values of the simulated fluctuations and mean flow.

The nonisotropy in the magnitude and structure of the turbulence shown in Figs. 3 and 4 suggests that typical isotropic turbulence models might omit critical aspects of the mixing in the interaction between the vegetation and mean flow. The roles and importance of this nonisotropy and its effects on fire spread should be investigated in future modeling and field observation research.

5.2. Fire propagation

Our LIVE fire simulation with mean canopy-top wind speeds of 2.52 m/s and 4.49 m/s illustrate the impact of wind speed on the fire's ability to propagate, which is consistent with earlier observations where fire spread in pinyon-juniper woodlands is often constrained at low wind speeds by sparse and heterogeneous fuels distribution. Bruner and Klebenow (1979) were able to successfully burn only 12 of 30 sites in pinyon-juniper woodlands in Nevada; they found that hot windy conditions were necessary to carry the fire between disjunct fuel pockets. Huffman et al. (2009) noted that low and poorly distributed fuel loads prevented fire spread in their northern Arizona pinyon-juniper study sites.

Fires in pinyon-juniper woodlands often do not propagate when winds are weak because surface fuels are not sufficient to carry the fire between the trees and thus the fire must largely move from tree to tree. In many locations, the trees are too far apart or the horizontal winds are too weak to lean the fire and hot combustion plume sufficiently into downwind trees. As a result, some portions of the fire do not propagate and eventually burn out, causing the fireline to fractionate. As the fractionated line moves downwind, new portions of the fireline arrive at gaps between trees that are too large for the wind speeds present at that location at that moment. This further fractionates the line until eventually the fireline goes out.

Wind fluctuations enhance fire spread to intermittently reach unburned fuel. Since the magnitude of the streamwise fluctuations scales with the mean flow velocity, these fluctuations likely contributed to spread in the LIVEHIGH simulation while the LIVELOW fire was extinguished. Another way that turbulence may affect sustainability of the fire in the LIVEHIGH simulation is through the lateral wind fluctuations, which also scale with the mean flow at the top of the canopy. Under LOW wind conditions the fireline becomes broken and in some cases goes out, whereas under HIGH winds the fires stay as more of a continuous fireline. It actually spreads slightly in the lateral direction in the DEADHIGH and DROPPEDHIGH scenarios. In these simulations, the firelines were broken soon after ignition as the fires began to spread, but the gaps in the line were healed and the firelines became continuous from the left to right before the fires reached the edge of the domain. Even the LIVEHIGH simulation is able to eventually achieve a fireline with minimal gaps in its length. This result is consistent with the notion that wind speed and crosswind fluctuations in the LIVEHIGH simulation play a role in enhancing forward movement of the fire in a diagonal fashion instead of being constrained to just downwind spread, as occurs when there are minimal lateral fluctuations. The formation of gaps in the firelines and in some cases, a steady decrease in the amount of active fireline, suggests that even though some of these fires are sustained at the simulated wind speeds once well established with long fire lines, they might not be able to grow from a point source.

Reduced moisture has first order effects in allowing the temperature of the foliage to increase faster because the radiative and convective energy are not used to heat and then evaporate as much water. This impacts fire spread by reducing the amount of energy needed to ignite unburned fuel, and decreasing the length of time that hot gases must pass through the unburned fuel in order to deposit needed energy. Thus, the DEAD scenario fires spread faster than the LIVE fires as expected. In situations where the fire and combustion gases are only intermittently blown into the unburned fuel, the result can be ignition or no ignition. Mean flow and turbulence can influence how moisture content affects fire spread, and contribute to the fact that the DROPPEDLOW fire can spread while the LIVELOW fire goes out.

Our simulations suggest that sparse fuels in pinyon-juniper woodlands can be overcome by decreasing canopy fuel moisture. Even under low wind speeds, dead needles on trees following high levels of bark beetle mortality allowed fires to propagate in the simulation. The low (15%) moisture content of the dead needles on the trees allows them to ignite more quickly than live needles with moisture contents of >80% (Jolly et al., 2012). It should be noted that if a less dense stand were simulated, the wind speed required for fire spread would be expected to increase even under DEAD conditions. Our results are similar to those of Hoffman et al. (2012b), who used WFDS simulations to investigate lodgepole pine forests in a similar scenario as our DEAD case. That study concluded that pre-outbreak forest structure and percent tree mortality influenced crown fire behavior when dead needles were in the crown, and that the effect varies with spatial heterogeneity of the trees.

The simulations of this study illustrate that fire spread in the sparse pinyon-juniper woodlands is also affected by dropping needles from the pinyon trees and thus increasing the amount of surface fine fuels. In addition to the effects on the canopy winds mentioned above, this redistribution of fuel limits the exposure of these fallen fuels to the fast moving air at the top of the canopy and greatly reduces the exposure of these fuels to strong vertical motions. When burning fuel is aloft in the canopy, winds accelerate vertically below them much as in a chimney, but the ground prevents this behavior in surface fuels. The result is reduced mixing, different heat-transfer mechanisms, and changed trajectories of hot gases. Even though the continuity of the surface fuels has not been altered when the needles are dropped, changes in the burn environment increase the ability of the fire to spread.

As expected, the reduction of moisture in just part of the canopy (since juniper trees were left at their original moisture levels) caused a profound increase in the spread rate, but this effect is more pronounced in the LOW wind case than the HIGH wind case, by factors of 2.59 vs. 1.83. The effects of opening up the canopy and increasing the dead fuel load on the ground caused a consistent slight decrease (factor of .88 and .89) in normalized spread rate compared to the LIVE cases. The differences in ROS speedup and slowdown factors indicate that the influences of moisture and vertical fuel distribution are not independent of wind speed at the top of the canopy. This is interesting in light of the fact that the wind profiles scaled linearly with the canopy top wind speed, indicating the nonlinear nature of the fire/atmosphere coupling.

The evolution in the AHRR of the simulated fires is consistent with other methods of looking at heat release, such as Byram (1959) empirical relationship that suggests heat release rate increases with the rate of spread of the fire. In addition to moving over unburned fuels at a faster rate, the faster ROS is also correlated with more active crown fire that consumes more canopy vegetation. The moisture levels in the canopy of the DEAD scenarios also contribute to increased heat release. The noticeable difference that wind speed makes in the AHRR per streamwise meter is indicative of the larger lateral extents and lower fragmentation of the fireline that occurs in the HIGH wind cases compared to the LOW wind scenarios.

6. Conclusions

Six simulations with a coupled fire/atmosphere model, FIRETEC, were performed with the intent of exploring some fundamental impacts of bark-beetle-induced pinyon tree mortality on fire behavior in pinyon-juniper woodlands. Fire spread in these discontinuous woodlands was strongly influenced by the advection of heat from one tree to another and subsequent convective heating, thus strongly influenced by the changes in canopy winds and turbulence. The balance between ambient winds and fire-induced buoyant flows determines the effectiveness of these processes in igniting new vegetation.

The various simulations represented three broad time periods in the evolution from live woodlands, to the period following bark beetle attack when trees have died but dead needles remain on the trees, to the period when dead pinyon needles fall to the ground. In all of these scenarios the juniper trees were alive and represented in the same way. Two different ambient wind speeds high above the stands were used to drive the fires. The simulated changes in fuel structure caused by the pinyon trees losing their needles alter the average wind profile as well as the wind fluctuations within the tree canopy. More specifically, the wind speeds in the canopy are lower when the needles are on the trees than when they are dropped, and the mean wind profile shapes and turbulence statistics are different.

The changes in canopy structure lead to changes in the fire spread rates through changes in fuel distribution (and thus the way fuels are ignited) and changes in the winds that push the fire. The differences in the mean wind speed in the vicinity of the canopy for the different canopy structures complicates direct comparison of spread rates for given wind speeds, since this relationship will be different for different heights. Spread rates normalized by the wind speeds at the top of the canopy facilitate comparison with less dependency on specific wind speeds. Since the winds at the elevations of the fuel and fire are most critical to fire spread, it is essential that fire scientists and fire practitioners are extremely careful in choosing the heights at which they measure wind for fire behavior predictions. Measuring winds above a canopy without accounting for disturbance-induced changes in wind profiles within the canopy can be very misleading.

It is also interesting to note that a simple function using total fuel load would not account for the variation in spread rates for a given wind speed since the total fuel load is the same in all of the simulations; only the moisture and spatial distribution changed. The relatively high tree density and tree mortality in our simulations resulted in a modified velocity profile and sufficiently high load of surface fine fuels (DROPPED simulation) to support fire propagation under the LOW wind condition. At lower levels of tree mortality, lesser degrees of wind penetration into the canopy and reduced fine fuel additions from dead needles may not be sufficient to sustain surface fire spread.

Varying wind speeds high above the canopy greatly altered simulated fire propagation. At the lower wind speed the fire in the live pinyon woodland goes out soon after ignition, whereas the fire under the higher wind conditions burns across the domain. These results suggest the presence of a threshold in fire behavior depending on the wind speed in the live pinyon woodland scenarios. The fact that the length of the active fireline decreases in all of the scenarios with lower ambient winds and the fireline actually grows in the scenarios with both dead pinyon trees and higher ambient winds, also suggests the potential of a less dramatic wind speed threshold in fire behavior in the presence of dead needles. Further research into the presence of these thresholds and the environmental conditions that control them is essential in light of the recent increase in prescribed and managed fires in this region.

Normalized spread rates are fastest for the scenarios where the pinyon needles are dead but still on the trees, and slowest after the dead needles are dropped. The differences between the various normalized spread rates are different for the two ambient wind speeds tested. This suggests the effects of canopy structure and canopy fuel moisture levels are nonlinear with wind speed, even though the wind profiles themselves appear to scale very well with ambient wind speed. The nonlinear interaction between canopy structure, atmosphere and fire also leads to changes in heat release as a function of downwind distance traveled with stand structure, moisture and wind speed. In the development of new operational models it will be important to account for these nonlinear interactions, and it is essential to find ways to observe and quantify these effects through field experiments.

The coupled interaction of the fire and atmosphere plays an important role in the fire behavior shown in these simulations. Much can be gained by using a coupled fire/atmosphere model to explore potential phenomenology that determines fire behavior response to changes in stand structure, such as that caused by bark-beetle induced tree mortality. This study should not be used as a definitive explanation of the fire-behavior response to such disturbances, but should instead help refine hypotheses that can be tested experimentally as well as guide data collection strategies.

Acknowledgments

This research was funded by National Fire Plan dollars as directed by USDA Forest Service, Rocky Mountain Research Station and Washington Office, Interagency Agreement 09-IA-11221633-215 with Los Alamos National Laboratory and Research Joint Venture 09-JV-11221633-325 with University of Idaho; USDA Forest Service, Forest Health Monitoring, Evaluation Monitoring grant INT-F-07-01; USDA Forest Service Southwestern Region, Forest Health; and Los Alamos National Laboratory. Los Alamos National Laboratory's Institutional Computing Program provided computational resources. Christian Hoffman and Christopher Looney helped collect and enter field data. We also thank the Apache-Sitgreaves, Coconino, and Kaibab National Forests for their support of this research.

Appendix 1. Wind in canopies

The fundamentals of wind interaction within forest canopies have been studied by a number of researchers. Basic wind-flow dynamics and turbulence over homogeneous (relatively continuous) canopies are reasonably well understood for neutral thermal stratification as being analogous to plane mixing-layer flow (Raupach et al., 1996). Mean wind fields in vegetation canopies are characterized by a strong shear at the canopy top associated with an inflection point in mean horizontal velocity, and a rapid decrease in turbulent kinetic energy and momentum flux from the top of the vegetation down into the canopy (see, for example, Brunet et al., 1994; Finnigan, 2000; Kaimal and Finnigan, 1994; Pimont et al., 2009; Raupach et al., 1996). The scale and magnitude of canopy heterogeneities affects the turbulence and mixing in the canopy, and momentum exchange between the winds above the vegetation and those within the canopy (Dupont and Brunet, 2006).

Wind-field characteristics within different types of continuous vegetation have been observed using in situ measurements and wind-tunnel experiments, such as those by Brunet et al. (1994), Finnigan (2000), Kaimal and Finnigan (1994), Raupach et al. (1986), and Shaw et al. (1988). Some of the effects of large discontinuities in forest structure (such as a road or fuel break) have been measured using wind-tunnel measurements (Raupach et al., 1987). In addition, various types of computational fluid dynamics (CFD) models have been used to simulate characteristics of winds in the presence of vegetated canopies, including several Reynolds-averaged Navier Stokes (RANS) type models (Foudhil et al., 2005; Green, 1992; Li et al., 1990; Liu et al., 1996). Large-eddy simulation (LES) techniques have been applied successfully over various homogeneous (Dupont and Brunet, 2008b; Kanda and Hino, 1994; Pimont et al., 2009; Shaw and Schumann, 1992; Su and Shaw, 2000; Su et al., 1998; Watanabe, 2004) and heterogeneous (Dupont and Brunet, 2008a; Patton et al., 1998; Yang et al., 2006a,b) vegetation canopies under neutral stratification.

RANS type models only simulate mean fields and average turbulent characteristics, and do not explicitly capture turbulent fluctuations within the canopy. However, dynamic wind fluctuations are likely to have significant effects on fire behavior within canopies. Thus, a RANS model might not be sufficient to capture the critical aspects of coupled fire/atmosphere behavior in discontinuous coniferous ecosystems. In contrast, LES techniques explicitly simulate transient motions of wind fields, resolving turbulent structures larger than twice the grid mesh and using subgrid-scale models to capture smaller eddy motions. Unfortunately, such LES tools have not yet been used to study the changes in wind penetration through highly discontinuous woodlands that result from insect mortally in part of the canopy.

In a wildfire context, the combined impacts of ambient winds above the vegetation, the turbulent mixing and coherent vortices that control the injection of horizontal momentum into the canopy, and the resulting shear profile within the canopy on fire behavior are not well understood. Yet, it seems likely that modification of these wind attributes post-insect attack would combine to influence fire propagation. Unfortunately, the lack of either in situ experiments or CFD efforts using LES focused on understanding winds in discontinuous vegetation types resembling pinyon-juniper woodlands in the southwestern US makes it difficult to assess the changes in fire behavior that would follow such an outbreak in these ecosystems.

Appendix 2. Conceptual model of fire spread in discontinuous woodlands

A simplified description of the modeled processes that lead to the ignition of unburned trees in front of a fire is provided in Fig. A1. As a fire approaches an unburned tree, radiative heat transfer begins to warm the portions of the tree that are facing the flame. As energy is deposited in the unburned tree, the temperature increases and some of the moisture near the surface begins to evaporate. As the temperature of the surface of the foliage and woody material of the tree increases, natural convection begins to extract energy from surfaces of the tree and carry this energy away via air currents. In this way, natural or forced convective heat transfer (in the presence of ambient winds) limits the temperature rise caused by slow but continuous heating from sources such as the sun or radiation from a flame some distance away. The effectiveness of convective cooling is higher for fine foliage particles than for larger objects such as tree trunks or buildings.

In instances where the hot combustion gases are carried through the unburned trees, convective cooling is interrupted and intense convective heating commences. In most cases, active combustion of previously unburned trees begins when both convective and radiative heating are present and convective cooling is absent. In this scenario, hot combustion gases from nearby burning ground or canopy fuels are advected (carried by fire-influenced winds) through the unburned trees. Fire propagation is accomplished by a combination of radiative and convective heating of unburned vegetation; however, the precise roles and balances of radiative and convective heat transfer in wildland fires is currently the subject of significant debate (Cohen and Finney, 2010). Resolution of these discussions is beyond the scope of this paper.

In pinyon-juniper woodlands, where there is minimal surface fuel between the trees, the probability of fire spreading from one tree to another is dependent on the distance between trees and the wind speeds within the woodland canopy. When the trees are closer together and/or the wind speeds are higher, the probability and rate of ignition of downwind trees is greater than for conditions where trees are farther apart and/or wind speeds are lower because gases are transported more vertically in lower-wind than higher-wind scenarios. When the flames and combustion gas plumes are angled more vertically (the flame angle in Fig. 1, θ, increases toward 90°), a shorter distance, d, can be bridged. In addition, heat is only convectively transferred in the direction of the wind. Therefore, crossstream wind fluctuations play a critical role in the sustainability of fire spread in discontinuous woodland ecosystems. The absence of such fluctuations only facilitates ignition of trees that are directly downwind, and thus reduces the chances that fire can spread laterally from tree-to-tree. As winds increase, the flames and

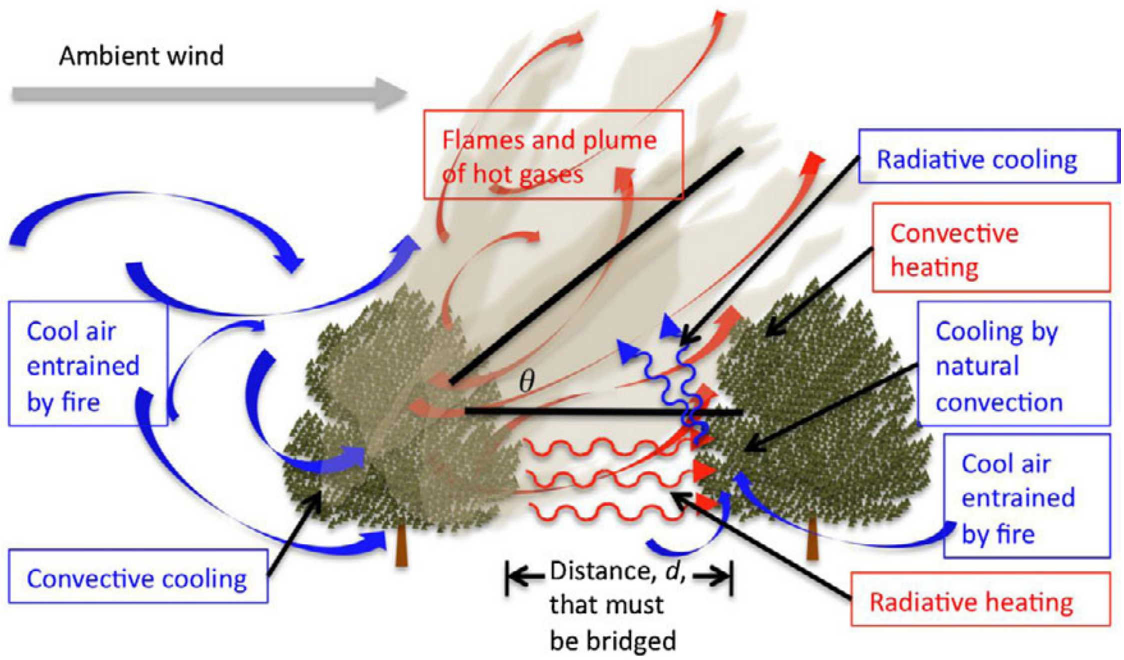

Fig. A1. Graphical description of conceptual model of processes that control the spread of fire to unburned vegetation in discontinuous woodland ecosystems.

plume are less vertical (θ decreases), the flames get stretched out, and the distance, *d*, that can be bridged between trees increases. As the strength and frequency of lateral fluctuations increases, the fire can spread more easily in directions other than directly downwind.

Appendix 3. Brief FIRETEC model description

FIRETEC was developed with the intention of modeling many of the critical physical phenomena that control the behavior of a wildfire and their interactions through a set of coupled partial differential equations. FIRETEC simulates the interaction between the physical processes by explicitly resolving many of them through a finite volume numerical solution algorithm, and stochastically representing fine-scale processes and heterogeneities that cannot be resolved in the numerical grid through subgrid models. A detailed description of the formulation and equation sets used in FIRETEC is provided in Dupuy et al. (2011). FIRETEC's representation of flow through forest canopies (although these canopies were of much higher cover fraction than those of pinyon-juniper woodlands) and in the presence of fuel discontinuities (namely clear cuts) have been shown to be realistic through comparison with the experiments of Shaw et al. (1988) and Raupach et al. (1987), respectively (Pimont et al., 2009). FIRETEC has been used to simulate historical fires (Bossert et al., 2000; Heller, 2002) and field experiments (Linn et al., 2005a, 2012a,b; Linn and Cunningham, 2005). Efforts to further validate FIRETEC for broader sets of scenarios are underway. FIRETEC has also been applied as a tool to study basic fire behavior phenomena (Cassagne et al., 2011; Cunningham and Linn, 2007; Dupuy et al., 2011; Linn et al., 2007, 2010, 2012b; Linn and Cunningham, 2005; Pimont et al., 2011, 2006). Applications of FIRETEC span ecosystems from sparse grass to heavily forested woodlands on both flat terrain and rugged topography, and include the interactions between fire and canopy structure as well as interactions between multiple firelines.

For this paper, we assume that the modeled interactions between critical processes such as wind flows and heat transfer modes in FIRETEC are adequate for this investigation based on previous FIRETEC investigations (Bossert et al., 2000; Heller, 2002; Linn et al., 2005a, 2012a,b; Linn and Cunningham, 2005; Pimont et al., 2009) where simulated fire behavior compared well with field observations (quantitatively and/or qualitatively). These studies do not constitute full validation of the model. However, they do illustrate that the balances of processes such as convective and radiative heat transfer in this model can result in realistic fire behavior. Therefore, for the purposes of this exploration, we assume that the modeled physics in FIRETEC also produces realistic fire spread behavior in pinyon-juniper woodlands, even though to date there have not been adequate observations or field experiments for validation of the model in these systems.

References

Allen, C.D., 2007. Interactions across spatial scales among forest dieback, fire, and erosion in northern New Mexico landscapes. Ecosystems 10, 797–808.

Bentz, B., et al., 2009. Bark Beetle Outbreaks in Western North America, Causes and Consequences. Bark Beetle Symposium. The University of Utah Press, Snowbird, Utah, 44 pp.

Bossert, J.E., et al., 2000. Coupled atmosphere-fire behavior model sensitivity to spatial fuels characterization. Third Symp. Fire Forest Meteorol., 21–26.

Breshears, D.D., et al., 2005. Regional vegetation die-off in response to global-change-type drought. Proc. Natl. Acad. Sci. U. S. A. 102 (42), 15144–15148.

Bruner, A.D., Klebenow, D.A.,1979. Predicting success of prescribed fires in pinyon-juniper woodland in Nevada Research Paper INT-219. USDA Forest Service, Nevada Agricultural Experiment Station, Ogden, UT, p. 20.

Brunet, Y., Finnigan, J.J., Raupach, M.R., 1994. A Wind-tunnel study of air-flow in waving wheat – single-point velocity statistics. Boundary-Layer Meteorol. 70 (1-2), 95–132.

Byram, G.M., 1959. Forest fire behavior. In: Davis, K.P. (Ed.), Forest Fire: Control and Use. McGraw-Hill Book Company, New York 36, pp. 90–123.

Cassagne, N., et al., 2011. Using a fire propagation model to assess the efficiency of prescribed burning in reducing the fire hazard. Ecol. Model. 222 (8), 1502–1514.

Clifford, M.J., Rocca, M.E., Delph, R., Ford, P.L., Cobb, N.S.,2008. Drought Induced Tree Mortality and Ensuing Bark Beetle Outbreaks in Southwestern Pinyon-Juniper Woodlands, Ecology, management, and restoration of pinon-juniper and ponderosa pine ecosystems: combined. In: Proceedings of the 2005 St. George, Utah and 2006 Albuquerque, New Mexico Workshops. U.S. Department of Agriculture, Forest Service, Rocky Mountain Research Station RMRS-P-51, St. George, Utah/Albuquerque, New Mexico, p. 13.

Cruz, M.G., Alexander, M.E., 2010. Assessing crown fire potential in coniferous forests of western North America: a critique of current approaches and recent simulation studies. Int. J.Wildland Fire 19 (4), 377–398.

Cunningham, P., Linn, R.R., 2007. Numerical simulations of grass fires using a coupled atmosphere-fire model: dynamics of fire spread. J. Geophys. Res.-Atmos. 112 (D5).

Derose, R.J., Long, J.N., 2009. Wildfire and spruce beetle outbreak: simulation of interacting disturbances in the central Rocky Mountains. Ecoscience 16 (1), 28–38.

Dupont, S., Brunet, Y., 2006. Simulation of turbulent flow in an urban forested park damaged by a windstorm. Boundary-Layer Meteorol. 120 (1), 133–161.

Dupont, S., Brunet, Y., 2008a. Edge flow and canopy structure: a large-eddy simulation study. Boundary-Layer Meteorol. 126 (1), 51–71.

Dupont, S., Brunet, Y., 2008b. Influence of foliar density profile on canopy flow: A large-eddy simulation study. Agric. Forest Meteorol. 148 (6–7), 976–990.

Dupuy, J.L., et al., 2011. Exploring three-dimensional coupled fire-atmosphere interactions downwind of wind-driven surface fires and their influence on backfires using the HIGRAD-FIRETEC model. Int. J. Wildland Fire 20 (6), 734–750.

Finnigan, J., 2000. Turbulence in plant canopies. Annu. Rev. Fluid Mech. 32, 519–571.

Cohen, J.D., Finney, M.A., 2010. An examination of fuel particle heating during fire spread. In: Viegas, D.X. (Ed.), Proceedings of the VI International Conference on Forest Fire Research; 15–18 November 2010. University of Coimbra, Coimbra, Portugal.

Floyd, M.L., et al., 2008. Fire history of pinon-juniper woodlands on Navajo Point, Glen Canyon National Recreation Area. Nat. Areas J. 28 (1), 26–36.

Foudhil, H., Brunet, Y., Caltagirone, J., 2005. A fine-scale k-epsilon model for atmospheric flow over heterogeneous landscapes. Environ. Fluid Mech. 5 (3), 247–265.

Green, S.R., 1992. Modelling turbulence air flow in a stand of widely-spaced trees, PHOENICS. J. Comput. Fluid Dyn. (5), 294–312.

Heller, A., 2002. This Model Can Take the Heat, Science & Technology Review. Lawrence Livermore National Laboratory, Lawrence Livermore National Laboratory, p. 36.

Hicke, J.A., Johnson, M.C., Hayes, J.L., Preisler, H.K., 2012. Effects of bark beetle-caused tree mortality on wildfire. Forest Ecol. Manag. 271, 81–90.

Hoffman, C.M., 2011. Numerical Simulation of Crown Fire Hazard in Bark Beetle Infested Lodgepole Pine Forests. Dissertation Thesis, University of Idaho, 97 pp.

Hoffman, C.M., et al., 2012a. Numerical simulation of crown fire hazard immediately after bark beetle-caused mortality in lodgepole pine forests. Forest Sci. 58 (2), 178–188.

Hoffman, C.M., Sieg, C.H., McMillin, J.D., Fule, P.Z., 2012b. Fuel loadings 5 years after a bark beetle outbreak in south-western USA ponderosa pine forests. Int.J. Wildland Fire 21, 306–312.

Huffman, D.W., Fule, P.Z., Crouse, J.E., Pearson, K.M., 2009. A comparison of fire hazard mitigation alternatives in pinyon-juniper woodlands of Arizona. Forest Ecol. Manag. 257 (2), 628–635.

Intergovernmental Panel on Climate Change (IPCC), 2007. Climate Change 2007: The Scientific Basis. Cambridge University Press, Boston, MA.

Jenkins, M.J., Hebertson, E., Page, W., Jorgensen, C.A., 2008. Bark beetles, fuels, fires and implications for forest management in the Intermountain West. Forest Ecol. Manag. 254 (1), 16–34.

Jenkins, M.J., Page, W.G., Hebertson, E.G., Alexander, M.E., 2012. Fuels and fire behavior dynamics in bark beetle-attacked forests in Western North America and implications for fire management. Forest Ecol. Manag. 275, 12.

Jolly, W.M., et al., 2012. Relationships between moisture, chemistry, and ignition of *Pinus contorta* needles during the early stages of mountain pine beetle attack. Forest Ecol. Manag. 269 (0), 52–59.

Kaimal, J.C., Finnigan, J.J., 1994. Atmospheric Boundary Layer Flows: Their Structure and Measurement. Oxford University Press, New York, 289 pp.

Kanda, M., Hino, M., 1994. Organized structures in developing turbulent-flow within and above a plant canopy, using large-eddy simulation. Boundary-Layer Meteorol. 68 (3), 237–257.

Keane, R.E., et al., 2008. Ecological effects of large fires on US landscapes: benefit or catastrophe? Int. J. Wildland Fire 17 (6), 696–712.

Li, Z.J., Lin, J.D., Miller, D.R., 1990. Air-flow over and through a forest edge – a steady-state numerical-simulation. Boundary-Layer Meteorol. 51 (1–2), 179–197.

Linn, R., et al., 2005a. Numerical simulations of fires similar to the International Crown Fire Modeling Experiment. In: Proceedings 6th Fire and Forest Meteorology Symposium and 19th Interior West Fire Council Meeting, Canmore, Alberta, Canmore, Alberta.

Linn, R., Winterkamp, J., Colman, J.J., Edminster, C., Bailey, J.D., 2005b. Modeling interactions between fire and atmosphere in discrete element fuel beds. Int. J. Wildland Fire 14 (1), 37–48.

Linn, R., Winterkamp, J., Edminster, C., Colman, J.J., Smith, W.S., 2007. Coupled influences of topography and wind on wildland fire behaviour. Int. J. Wildland Fire 16 (2), 183–195.

Linn, R.R., 1997. A Transport Model for Prediction of Wildfire Behavior. LA-13334-T. Los Alamos National Laboratory, Los Alamos, NM.

Linn, R., Anderson, K., Winterkamp, J., Brooks, A., Wotton, M., Dupuy, J.-L., Pimont, F., Edminster, C., 2012a. Incorporating field wind data into FIRETEC simulations of the International Crown Fire Modeling Experiment (ICFME): preliminary lessons learned. Can. J. For. Res. 42, 879–898, http://dx.doi.org/10.1139/X2012-038.

Linn, R.R., et al., 2012b. Using periodic line fires to gain a new perspective on multi-dimensional aspects of forward fire spread. Agric. Forest Meteorol. 157 (0), 60–76.

Linn, R.R., Cunningham, P., 2005. Numerical simulations of grass fires using a coupled atmosphere-fire model: basic fire behavior and dependence on wind speed. J. Geophys. Res. D-Atmos. 110 (D13).

Linn, R.R., Winterkamp, J.L., Weise, D.R., Edminster, C., 2010. A numerical study of slope and fuel structure effects on coupled wildfire behaviour. Int. J. Wildland Fire 19 (2), 179–201.

Liu, J., Chen, J.M., Black, T.A., Novak, M.D., 1996. E-epsilon modelling of turbulent air flow downwind of a model forest edge. Boundary-Layer Meteorol. 77 (1), 21–44.

Mell, W., Jenkins, M.A., Gould, J., Cheney, P., 2007. A physics-based approach to modelling grassland fires. Int. J. Wildland Fire 16 (1), 1–22.

Mell, W., Maranghides, A., McDermott, R., Manzello, S.L., 2009. Numerical simulation and experiments of burning douglas fir trees. Combust. Flame 156 (10), 2023–2041.

Miller, R.F., Svejcar, T.J., Rose, J.A., 2000. Impacts of western juniper on plant community composition and structure. J. Range Manag. 53 (6), 574–585.

Miller, R.F., Wigand, P.E., 1994. Holocene changes in semiarid pinyon-juniper woodlands. Bioscience 44 (7), 465–474.

Page, W., Jenkins, M.J., 2007a. Predicted fire behavior in selected mountain pine beetle-infested lodgepole pine. Forest Sci. 53 (6), 662–674.

Page, W.G., Jenkins, M.J., 2007b. Mountain pine beetle-induced changes to selected lodgepole pine fuel complexes within the intermountain region. Forest Sci. 53 (4), 507–518.

Parsons, R.A., 2007. Spatial Variability in Forest Fuels: Simulation Modeling and Effects on Fire Behavior. Dissertation Thesis, University of Montana, 268 pp.

Patton, E.G., Shaw, R.H., Judd, M.J., Raupach, M.R., 1998. Large-eddy simulation of windbreak flow. Boundary-Layer Meteorol. 87 (2), 275–306.

Perry, G.L.W., 2004. SpPack: spatial point pattern analysis in Excel using Visual Basic for Applications (VBA). Environ. Model. Software 19 (6), 559–569.

Pimont, F., Dupuy, J.-L., Linn, R.R., Dupont, S., 2009. Validation of FIRETEC wind-flows over a canopy and a fuel-break. Int. J. Wildland Fire 18 (7), 775–790.

Pimont, F., Dupuy, J.-L., Linn, R.R., Dupont, S., 2011. Impacts of tree canopy structure on wind flows and fire propagation simulated with FIRETEC. Ann. Forest Sci. 68 (3), 523–530.

Pimont, F., Linn, R.R., Dupuy, J.L., Morvan, D., 2006. Effects of vegetation description parameters on forest fire behavior with FIRETEC. Forest Ecol. Manag. 234S (S120).

Raupach, M.R., Bradley, E.F., Ghadiri, H., 1987. A Wind Tunnel Investigation into Aerodynamic Effect of Forest Clearing on the Nesting of Abbott's Boody on Christmas Island. Csiro Centre for Environmental Mechanics, Canberra.

Raupach, M.R., Coppin, P.A., Legg, B.J., 1986. Experiments on Scalar Dispersion Within A Model-plant Canopy. 1. The Turbulence Structure. Boundary-Layer Meteorol. 35 (1–2), 21–52.

Raupach, M.R., Finnigan, J.J., Brunet, Y., 1996. Coherent eddies and turbulence in vegetation canopies: The mixing-layer analogy. Boundary-Layer Meteorol. 78 (3–4), 351–382.

Roccaforte, J.P., Fule, P.Z., Covington, W.W., 2008. Landscape-scale changes in canopy fuels and potential fire behaviour following ponderosa pine restoration treatments. Int. J. Wildland Fire 17 (2), 293–303.

Romme, W.H., et al., 2009. Historical and modern disturbance regimes, stand structures, and landscape dynamics in pinon-juniper vegetation of the Western United States. Rangeland Ecol. Manag. 62 (3), 203–222.

Romme, W.H., et al., 2006. Recent Forest Insect Outbreaks and Fire Risk in Colorado Forests: A Brief Synthesis of Relevent Research, Colorado State University. Fort Collins, Colorado, USA.

Rothermel, R.C.,1972. A mathematical model for predicting fire spread in wildland fuels Research Paper INT-115. U.S. Department of Agriculture, Forest Service, Intermountain Forest and Range Experiment Station, Ogden, UT, p. 40.

Rothermel, R.C.,1983. How to Predict the Spread and Intensity of Forest and Range Fires GTR-INT-143. U.S. Department of Agriculture, Forest Service, Intermountain Forest and Range Experiment Station, Ogden, UT, p. 166.

Rothermel, R.C.,1991. Predicting behavior and size of crown fires in the Northern Rocky Mountains Research Paper INT-438. U.S. Department of Agriculture, Forest Service, Intermountain Research Station, Ogden, UT, p. 46.

Schmid, J.M., Amman, G.D., USDA,1992. Dendroctonus Beetles and Old-growth Forests in the Rockies, GTR-RM-213. In: Old-Growth Forests in the Southwest and Rocky Mountain Regions: Proceedings of a Workshop. U.S. Department of Agriculture, Forest Service, Fort Collins, CO, pp. 51–59.

Shaw, J.D., Steed, B.E., DeBlander, L.T., 2005. Forest Inventory and Analysis (FIA) annual inventory answers the question: What is happening to pinyon-juniper woodlands? J. Forest. 103 (6), 280–285.

Shaw, R.H., Denhartog, G., Neumann, H.H., 1988. Influence of foliar density and thermal-stability on profiles of reynolds stress and turbulence intensity in a deciduous forest. Boundary-Layer Meteorol. 45 (4), 391–409.

Shaw, R.H., Schumann, U., 1992. Large-eddy simulation of turbulent-flow above and within a forest. Boundary-Layer Meteorol. 61 (1-2), 47–64.

Simard, M., Romme, W.H., Griffin, J.M., Turner, M.G., 2010. Do mountain pine beetle outbreaks change the probability of active crown fire in lodgepole pine forests? Ecol. Monogr. 81 (1), 3–24.

Stimson, H.C., Breshears, D.B., Ustin, S.L., Kefauver, S.C., 2005. Spectral sensing of foliar water conditions in two co-occurring conifer species: *Pinus edulis* and *Juniperus monosperma*. Remote Sensing Environ. 96, 108–118.

Su, H.B., Shaw, R.H., Paw, U.K.T., 2000. Two-point correlation analysis of neutrally stratified flow within and above a forest from large-eddy simulation. Boundary-Layer Meteorol. 94 (3), 423–460.

Su, H.B., Shaw, R.H., Paw, U.K.T., Moeng, C.H., Sullivan, P.P., 1998. Turbulent statistics of neutrally stratified flow within and above a sparse forest from large-eddy simulation and field observations. Boundary-Layer Meteorol. 88 (3), 363–397.

Van Wagner, C.E., 1977. Conditions for the Start and Spread of Crown Fire. Can. J. Forest Res. 7 (1), 23–34.
Watanabe, T., 2004. Large-eddy simulation of coherent turbulence structures associated with scalar ramps over plant canopies. Boundary-Layer Meteorol. 112 (2), 307–341.
Westerling, A.L., Hidalgo, H.G., Cayan, D.R., Swetnam, T.W., 2006. Warming and earlier spring increase western US forest wildfire activity. Science 313 (5789), 940–943.
Yang, B., Morse, A., Shaw, R., Paw, U.K., 2006a. Large-eddy simulation of turbulent flow across a forest edge. Part II: momentum and turbulent kinetic energy budgets. Boundary-Layer Meteorol. 121 (3), 433–457.
Yang, B., et al., 2006b. Large-eddy simulation of turbulent flow across a forest edge. Part I: Flow statistics. Boundary-Layer Meteorol. 120 (3), 377–412.